01 Jan 2007

A New Inverter for Improved Fuel Cell Performance in Grid-Tied Application

Nagasmitha Akkinapragada

Badrul H. Chowdhury
Missouri University of Science and Technology, bchow@mst.edu

A New Inverter for Improved Fuel Cell Performance in Grid-tied Application

Nagasmitha Akkinapragada, *Student Member, IEEE,* and Badrul H. Chowdhury, *Senior Member, IEEE*

***Abstract*—The interconnection of a solid oxide fuel cell (SOFC) with the power conditioning units vis-à-vis a DC/DC converter and a DC/AC inverter for interfacing with the utility grid is presented. Fuel cells operate at low voltages and hence need to be boosted and inverted in order to be connected to the grid. The fuel cell and the DC/DC converter modeling are briefly explained. The methodology and the controller design for the control of power flow from the fuel cell to the utility grid are discussed. Power characteristics of the DC/AC inverter are compared with the characteristics of the DC/DC converter and the fuel cell. Fuel cells have slow response time which prevents it from grid-tie applications. Simulations validate the improvement in the response when the power conditioning unit is connected.**

***Index Terms*—SOFC, DC/DC converter, DC/AC inverter, real and reactive power control, distributed generation.**

I. Introduction

HIGH TEMPERATURE fuel cells such as the solid oxide fuel cell (SOFC) have the potential for centralized power generation, distributed power generation as well as combined heat and power. Compared to the other fuel cells, SOFCs are capable of handling more convenient forms of hydrocarbon fuels; they are highly efficient; and tolerant to impurities and its high temperature enables internal reforming. SOFC is a fast growing technology. There are various companies involved in research and development of tubular solid oxide fuel cell systems [1]. Siemens-Westinghouse Power Corp. has developed it first prototype of 125kW system for cogeneration applications and is in the process of commercialization. GE global research has successfully developed a 6kW prototype of SOFC system with the support of U.S. DOE for testing purposes. Accumentrics Corporation has installed a 5kW SOFC system near Cleveland, Ohio. This unit is being operated in a grid-parallel mode but also has the additional capability of operating in an independent island mode. They are working on commercialization.

Fuel cells operate at low DC voltages which need to be boosted (DC/DC converter) and inverted (DC/AC inverter) in order to be connected to the utility grid or operated in stand-alone applications. The SOFC and the DC/DC converter dynamic models have been discussed in [2]. The voltage source inverter (VSI) modeling and the associated control methodologies are further discussed in this paper. The VSI plays a vital role in interfacing the fuel cell-DC/DC system with the utility grid. This is due to the fact that the inverter switching control determines the direction of the power flow from the fuel cell system to the grid. Various strategies have been proposed earlier, based on the real and reactive power control [3]-[6]. The proposed strategy also involves real and reactive power control to obtain the desired phase angle and modulation index respectively. The technique proposed in this paper follows a slightly different methodology compared to the techniques proposed earlier. The control scheme in this paper also has PI controllers as in the previous references but differs in terms of determination of the duty cycle signals. The method followed to compute the duty cycle terms is shown in section III. Sine-triangle modulation is used to determine the switching signals for the three phase inverter. Fig. 1 shows the block diagram representation of the fuel cell system connected to the utility grid.

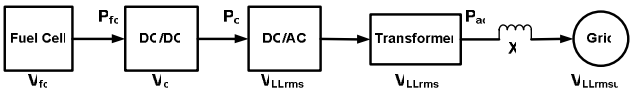

Fig.1 Fuel Cell system

Where,
V_{fc}: Fuel cell stack voltage (V)
V_o: Output voltage of DC/DC converter (V)
V_{LLrmsi}: Output voltage of the three phase inverter (V)
V_{LLrmst}: Voltage across the transformer (kV)
K_t: Turns ratio of the transformer
X_t: Leakage reactance of the transformer (Ω)
V_{LLrmsu}: Utility grid voltage (kV)

The following assumptions have been made in this system:

- Switching losses of the inverter are neglected.
- The three phase transformer is assumed to be ideal and modeled accordingly.
- Transformer has been considered to be ideal. Voltage across the transformer is modeled as turns ratio times the voltage on the inverter side and the leakage reactance in series with it [4].
- Reactive power is taken as zero (Q=0).

Section II deals with a brief description of the SOFC and

This work was supported in part by the U.S. National Science Foundation under Grant ECS-0523897.

Both authors are with the Electrical & Computer Engineering department of the University of Missouri, Rolla, MO 65401. Email: bchow@umr.edu.

the DC/DC converter model. The inverter modeling has been discussed in detail in this section. Section III deals with the controller design and the associated equations and subsystems. Section IV contains the simulation results and section V concludes the paper.

II. DYNAMIC MODELS

A. THE SOLID OXDE FUEL CELL

The SOFC is a high temperature operating fuel cell which has high potential in stationary applications. It is solid-state device that uses an oxide ion-conducting non-porous ceramic material as the electrolyte [7]. High temperature operation removes the need for precious-metal catalyst, thereby reducing cost. It also allows SOFCs to reform internally, which enables the use of a variety of fuels and reduces the cost associated with adding a reformer to the system [2].Two different geometries which are being developed are tubular and planar. The tubular design is the most advanced and is slated for large commercial and industrial cogeneration applications and onsite power generation [8].

A simulation model is developed for the SOFC in PSCAD based on the model and the parameters from ref [9]. Fig. 2 shows the typical volt-amp characteristics of the SOFC. Fuel cells have drooping characteristics: an increase in the load current causes a decrease in the stack voltage. The number of cells is taken to be 384 and the standard cell potential is 1.18V (from ref [9]). Hence the open circuit voltage (OCV) is 453V which decreases as the load current increases as seen in Fig. 2. The voltage drops rapidly at lower and higher currents. The drop is fairly linear in the middle region which is the operating region for the fuel cell.

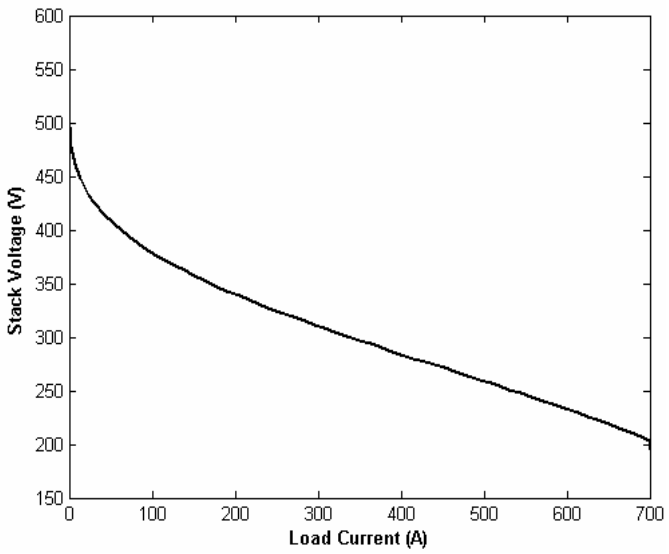

Fig. 2 Volt-amp characteristics of SOFC.

B. DC/DC CONVERTER

The main drawback of fuel cells is that they have a long thermodynamic time constant due to which the fuel cells cannot respond immediately to load changes or transients. Further, fuel cells operate at low voltages which need to be boosted to a higher level in order to be connected to the utility grid. A non isolated buck-boost converter has been used to obtain higher range of input voltage control and smoother output voltage. Fig. 3 shows the circuit diagram of the non-isolated DC/DC buck-boost converter

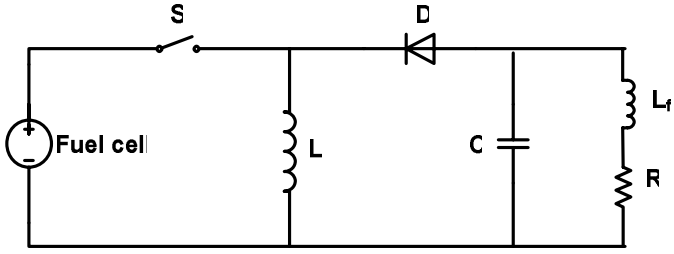

Fig. 3 Non-isolated DC/DC Buck-boost converter [10]

The switching control of the converter has been discussed in detail in [2] and will not be discussed in this paper. Fig. 4 shows the voltage characteristics of the fuel cell and the converter. The reference voltage has been set at 600V. For a step change in the reference power (50 to 90 kW), there is a decrease in the fuel cell stack voltage. The stack voltage takes around 5s to change from 420 to 390V due to the long thermodynamic constant of the fuel cell. The duty cycle control of the DC/DC converter operates to maintain the output voltage constant at the reference value (i.e. 600V). Despite the change in the stack voltage, the output voltage across the DC/DC converter is maintained constant at the commanded value of 600V as shown in Fig. 4.

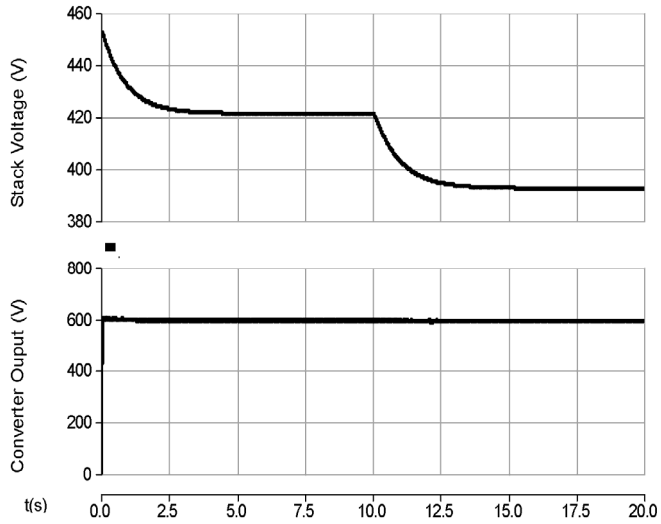

Fig. 4 Voltage characteristics of fuel cell and the converter for a step change in the reference power (50 to 90 kW).

C. DC/AC INVERTER

A three phase six-switch PWM VSI is used to convert the power available at the dc bus to ac power. The switching signals are obtained from the real and the reactive power control system. Fig. 5 shows the three-phase DC/AC voltage

source inverter connected to the infinite source (utility grid) through a transformer and a coupling reactance.

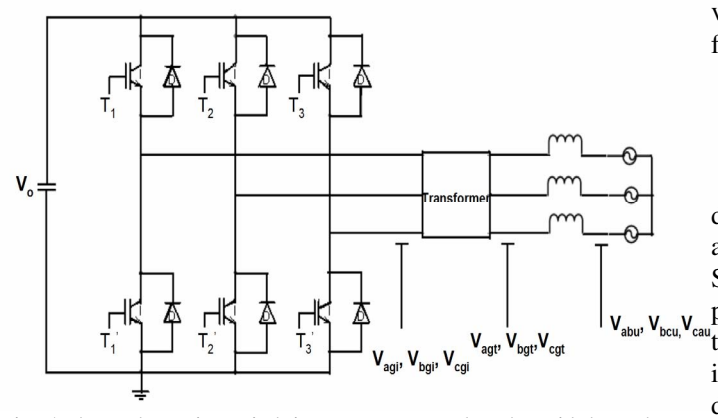

Fig. 5 Three phase six–switch inverter connected to the grid through a transformer

V_o : DC voltage from the DC/DC converter
T_1-T_3 : Transistor (switching) signals
V_{agi}, V_{bgi}, V_{cgi} : Line to ground voltages on the inverter side
V_{agt}, V_{bgt}, V_{cgt} : Line to ground voltages on the transf. side
V_{abu}, V_{bcu}, V_{cau} : Line to line voltages on the utility side

The switching loses of the inverter are neglected. The three phase inverter is modeled as an ideal inverter.

$$\begin{pmatrix} V_{agi} \\ V_{bgi} \\ V_{cgi} \end{pmatrix} = V_o \begin{pmatrix} 1 & 0 & 0 \\ 0 & 1 & 0 \\ 0 & 0 & 1 \end{pmatrix} \cdot \begin{pmatrix} T_1 \\ T_2 \\ T_3 \end{pmatrix} \quad (1)$$

Eq. (1) is used to model the three phase inverter. The line-neutral voltages on the inverter side are determined using the following equation.

$$\begin{pmatrix} V_{ai} \\ V_{bi} \\ V_{ci} \end{pmatrix} = \frac{1}{3} \begin{pmatrix} 2 & -1 & -1 \\ -1 & 2 & -1 \\ -1 & -1 & 2 \end{pmatrix} \cdot \begin{pmatrix} V_{agi} \\ V_{bgi} \\ V_{cgi} \end{pmatrix} \quad (2)$$

The transformer has been modeled as an ideal transformer with turns ratio (K_t) in series with its leakage inductance (L_t) [4]. The transformer side line-neutral voltages are given by the following equation.

$$\begin{pmatrix} V_{at} \\ V_{bt} \\ V_{ct} \end{pmatrix} = K_t \cdot \begin{pmatrix} V_{ai} \\ V_{bi} \\ V_{ci} \end{pmatrix} \quad (3)$$

The line-line rms voltage (V_{LLrmst}) on the transformer side is calculated using the line-neutral voltages. The line-ground voltages on the utility side are measured from the system. Eq (2) is used to calculate the line-neutral voltages on the utility side (use subscript 'u' instead of 'i') and then the line-line rms voltage (V_{LLrmsu}) is determined. These voltages are required for calculating the real and reactive power.

III. DESIGN OF CONTROLLER FOR THE INVERTER

The control scheme proposed in this paper is the decoupled PQ control. This controller controls the phase angle and amplitude of the voltage across the transformer. Since the phase angle of the voltage on the utility side is zero, phase angle of the voltage across the transformer determines the direction of the power flow. The reactive power injection into the grid is assumed to be zero. Fig. 6 shows the block diagram of the overall inverter control sub-system. The figure consists of various sub blocks to be dealt with, apart from the P-Q controller. These blocks are discussed in detail next.

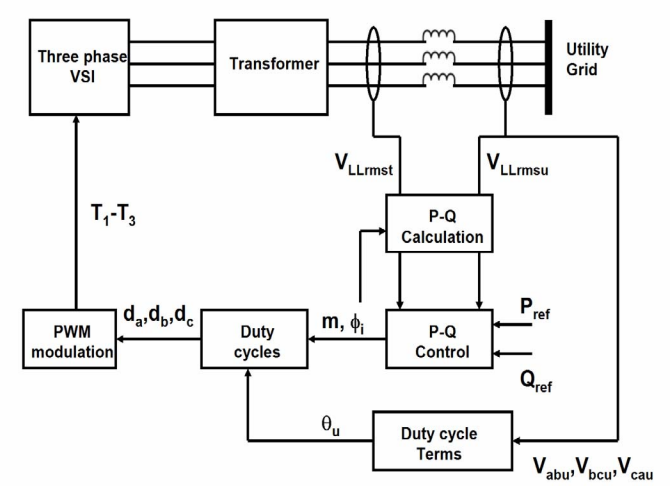

Fig. 6 Block diagram of the overall control system of the inverter

A. P Q Calculation

The line-line rms voltage (V_{LLrmsu}) on the utility side is measured from the system. The line-line rms voltage (V_{LLrmst}) on the transformer side is determined using Eqs. (1-3). The real and reactive power flow equations are given as follows:

$$P = \frac{V_{LLrmst} \cdot V_{LLrmsu} \cdot \sin(\phi_i)}{X_t} \quad (4)$$

$$Q = V_{LLrmst} \left(\frac{V_{LLrmst} - V_{LLrmsu} \cdot \cos(\phi_i)}{X_t} \right) \quad (5)$$

$$X_t = \omega L_t \quad (6)$$

Where ϕ_i is the phase angle of the voltage on the inverter side. and L_t is the leakage inductance of the transformer. Since the transformer is considered to be ideal, the angle lag due to the Y-Δ connection is neglected.

B. P-Q Control

The main components required for the inverter control

(i.e. switching signals) is the phase angle of the inverter and the modulation index. The utility side angle is considered to be zero (for an infinite bus). The difference in the angles determines the direction of the power flow. The real power flow is given by Eq. (4). The voltages and the reactance terms are more or less constant. The real power is directly proportional to the phase angle if the angle is small. Hence the real power flow can be used to control the phase angle of the inverter. Fig. 7 shows the real and reactive power control system. The error between the reference and the measured real power is fed into a PI controller to control the phase angle of the inverter. The inverter voltage is used to determine the amplitude of the modulation signals. The voltage in turn depends on the reactive power. The error between the reference and the measured reactive power is fed into a PI controller. The output of the controller is summed with the term $V_{LLrmsu}\cos(\phi_i)$ based on Eq. (5) to obtain the voltage on the transformer side. The control of the transformer voltage is proportional to the control of the inverter voltage. The modulation index is given by the following equation:

$$m = V_{LLrmst}\cdot\sqrt{\frac{2}{3}}\cdot\frac{2}{V_o}\cdot\frac{1}{K_t} \tag{7}$$

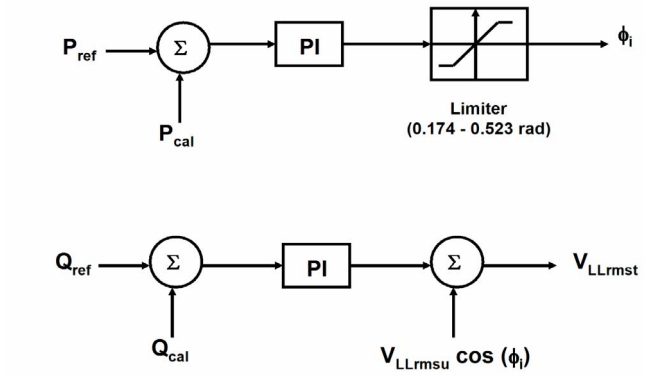

Fig. 7 Real and reactive power control system.

C. *Duty Cycle signals*

The duty cycle control signals are given by Eq. (8) [11]. These control signals are compared with the triangular wave (of switching frequency 1000 Hz) to determine the switching signals for the inverter. These switching signals are used to determine the inverter voltages.

$$d_a = \frac{1}{2}\left(1 + m\cdot\cos\left(\theta_u + \phi_i\right) - \frac{m}{6}\cos\left(3\theta_u + 3\phi_i\right)\right)$$

$$d_b = \frac{1}{2}\left(1 + m\cdot\cos\left(\theta_u + \phi_i - 2\frac{\pi}{3}\right) - \frac{m}{6}\cos\left(3\theta_u + 3\phi_i\right)\right) \tag{8}$$

$$d_c = \frac{1}{2}\left(1 + m\cdot\cos\left(\theta_u + \phi_i + 2\frac{\pi}{3}\right) - \frac{m}{6}\cos\left(3\theta_u + 3\phi_i\right)\right)$$

Phase angle (ϕ_i) and modulation index (m) are determined in subpart (B). The trigonometric terms expressed in terms of θ_u can be determined using the line-line voltages on the utility side. These line-line voltages on the utility side can be expressed in equation form as follows.

$$V_{abu} = \sqrt{3}\,V_u \sin\left(\theta_u + \frac{\pi}{6}\right)$$

$$V_{bcu} = -\sqrt{3}\,V_u \cos\left(\theta_u\right) \tag{9}$$

$$V_{cau} = -\sqrt{3}\,V_u \sin\left(\theta_u - \frac{\pi}{6}\right)$$

Where V_u is the peak value of the line-neutral voltage and θ_u is the utility side phase angle. This peak value can be determined using the line-line voltages, given by the following equation.

$$V_u = \frac{2}{3}\cdot\sqrt{V_{abu}^{\,2} + V_{bcu}^{\,2} + V_{abu}\cdot V_{bcu}} \tag{10}$$

Eq. (9) can be re-written as follows:

$$\sin\left(\theta_u + \frac{\pi}{6}\right) = \frac{V_{abu}}{\sqrt{3}\,V_u}$$

$$\cos\left(\theta_u\right) = \frac{-V_{bcu}}{\sqrt{3}\,V_u} \tag{11}$$

$$\sin\left(\theta_u - \frac{\pi}{6}\right) = \frac{-V_{cau}}{\sqrt{3}\,V_u}$$

The line-line voltages are measured from the system and V_u is calculated using Eq. (10). Eq. (11) is used to determine the other terms required in calculating the duty cycle signals.

IV. Constraints

The following constraints have been made for simulating the fuel cell power system.

Constraints:

1) $V_{LLrmsi} \le \frac{V_o}{\sqrt{2}}$ i.e., $V_{LLrmsi} \le 424.26\,V$

$$V_{LLrmst} = K_t \cdot V_{LLrms}$$

$$V_{LLrmst} \le 30.6 \times 426.2 \text{(} \quad \text{i.e.,} \quad V_{LLrmst} \le 12.9 \text{ V}$$

2) The third harmonic injection increases the range of modulation index. Without the injection, the range is between 0 and 1. With the injection, the range is:

$$0 < m < 1.15$$

3) Reactive power is considered to be zero (Q=0). Eq. (5) is reduced to the equation given below:

$$V_{LLrmst} = V_{LLrmsu} \cdot \cos(\phi_i) \tag{12}$$

Further, the phase angle is limited to 30^o (0.523 radians) in order to provide linear power control [12]. The limitation on the phase angle leads to the following inequality.

$$V_{LLrmst} \le 12.5 \times 10^3 \text{ V} \tag{13}$$

The fuel cell system has been simulated using these constraints. The system data is given in Table 1. in the appendix.

V. RESULTS

A. *Commanded P_{ref} of 50 kW*

A reference real power of 50 kW is commanded in order to test the proper functioning of the PQ control system. The voltage characteristics of the fuel cell system have been plotted below. Assumptions made in the system are given in Table 1 in the appendix. For a reference power of 50 kW, the fuel stack voltage is around 420 V, the output voltage of the DC/DC converter is 600 V. The stack voltage takes around 5s to reach to a steady value where as the voltage across the DC/DC converter takes less than 0.1s to reach the steady state value. Fig. 8a shows the voltage characteristics of fuel cell and DC/DC converter.

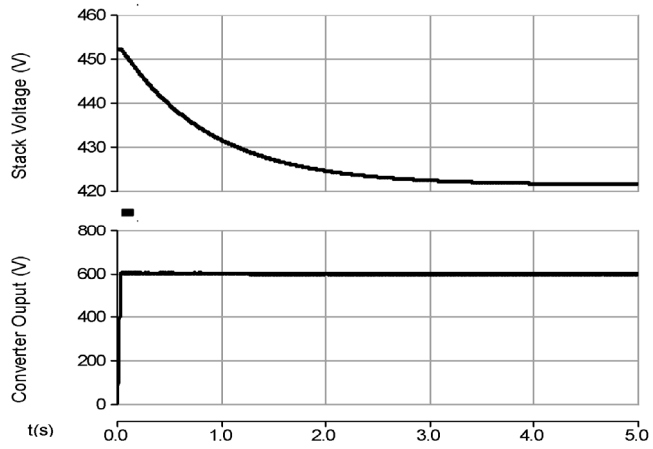

Fig. 8a Voltage characteristics of the fuel cell and the DC/DC converter for a P_{ref} of 50 kW

Fig. 8b shows the line-neutral voltage across the transformer and the utility side. As per the assumptions given in the appendix, the line-line rms voltage on the utility side is 12.5kV. Therefore the line-neutral (peak) voltage is 10.2kV which can be seen in Fig. 9b. According to the constraint given by Eq. (13), line-line rms voltage across the transformer should be less than 12.5kV which implies that the line-neural (peak) value should be less than 10.2kV. The peak value of voltage across the transformer is 9.9kV as seen in Fig. 8b.

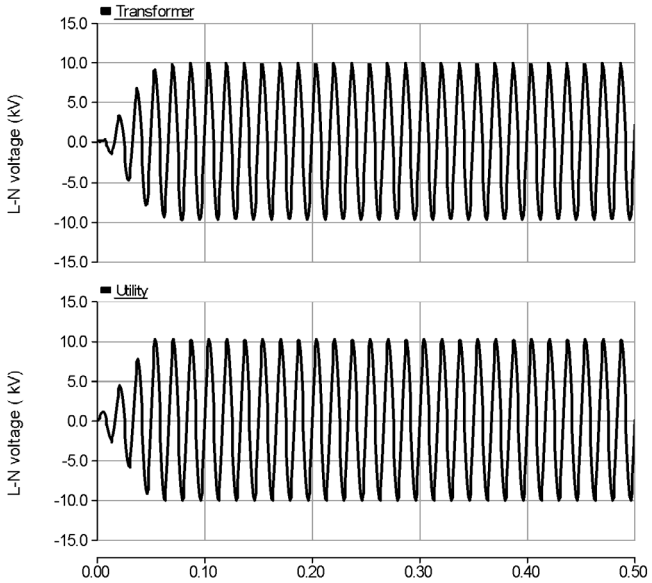

Fig. 8b Line-neutral voltages across transformer and the utility

Fig. 9 shows the real and reactive power characteristics. The real power reaches to the commanded value of 50 kW in less than 0.1s. In this system, reactive power injection is assumed to be zero and it is evident from Fig. 9.

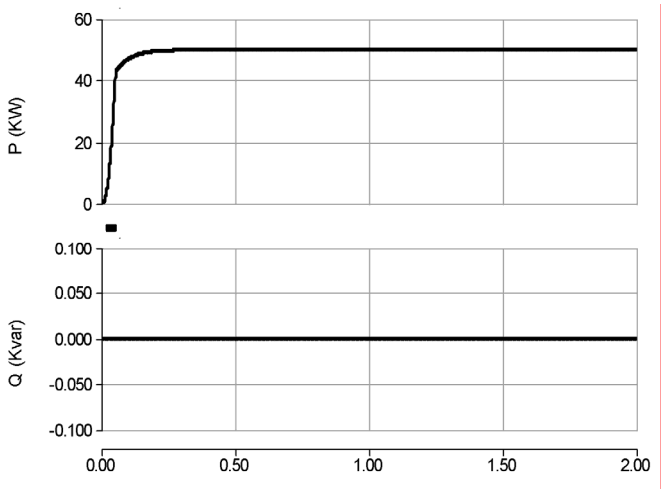

Fig. 9 Real and reactive power flow from the inverter to the utility

Fig. 10 shows the phase angle of the inverter and modulation index obtained from the PQ control. For a reference real power of 50 kW and with the assumptions made, the phase angle of the inverter (ϕ_i) and the modulation index is 0.2195 radians and 1.08 respectively.

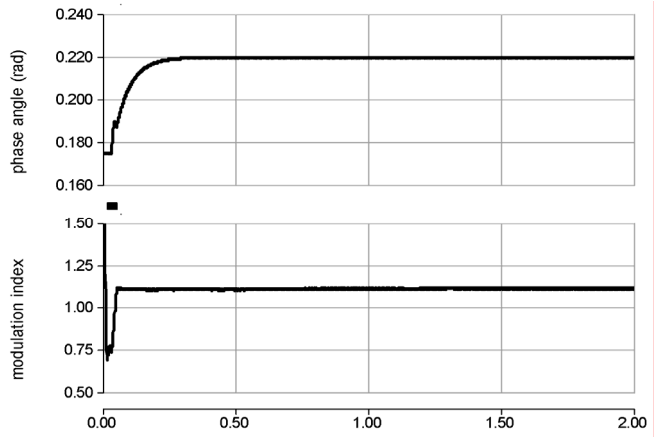

Fig. 10 Phase angle and modulation index from the PQ control

B. Step change in P_{ref}

A step change in the real reference power is considered in the entire system. The voltage and power characteristics are plotted. The control variables (phase angle and the modulation index) are also plotted for a step change in reference power from 50 to 90 kW. There is no reactive power injection. For a step change in P_{ref}, the fuel cell stack voltage decreases gradually from 420 to 390V. The stack current and the fuel cell power increase from 120 to 230A and 50 to 90kW respectively. Fig. 11 shows the fuel cell characteristics. Voltage, current and power take around 5s to reach the new steady value after the step change in the reference power (slow response of the fuel cell).

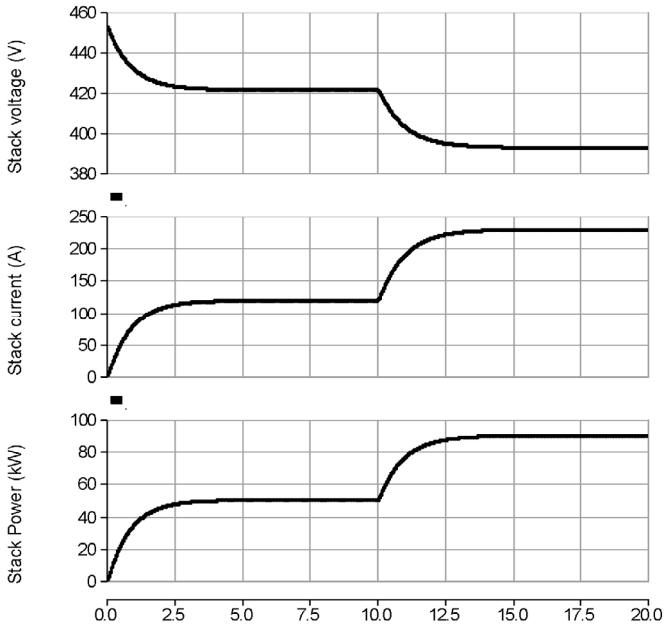

Fig. 11 SOFC characteristics

Fig. 12 shows the DC/DC converter characteristics. For the step change in the real power, the DC output voltage V_O is maintained at 600 V with the duty cycle control system. The converter current and power increase from 80 to 150A and 50 to 90kW. Despite the change in the stack voltage, the voltage across the converter is maintained constant at the commanded value of 600V. The power output and the current of the converter reach the new steady value in lesser time compared to the fuel cell power and current which is evident from Fig. 12. The response time is slightly improved with the DC/DC converter (from 5 to 2.5s).

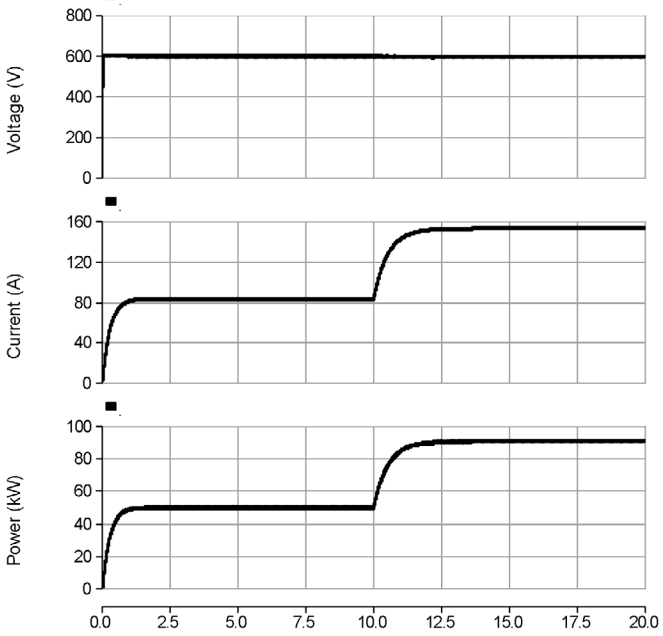

Fig. 12 DC/DC converter characteristics

Fig. 13 shows the real and reactive power characteristics at the output of the transformer for the step change in P_{ref}. The real power takes less than 0.1s to reach the new steady value. The reactive power injection is assumed to be zero and this is evident from the characteristics.

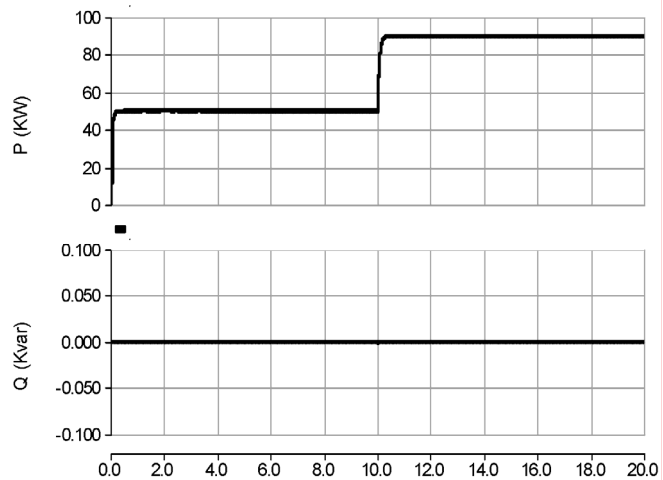

Fig. 13 Real and reactive power injections for step change in P_{ref} from 50 to 90kW

Fig. 14 shows the plots of the control variables (phase angle and the transformer voltage) obtained from the PQ control system. The modulation index is determined from the amplitude of the transformer voltage. For a step change in P_{ref} (50 to 90kW), the phase angle increases from 0.2195 to 0.4356 radians and the transformer voltage decreases from

12.2 to 11.3kV. Consequently, the modulation index decreases from 1.08 to 1.01.

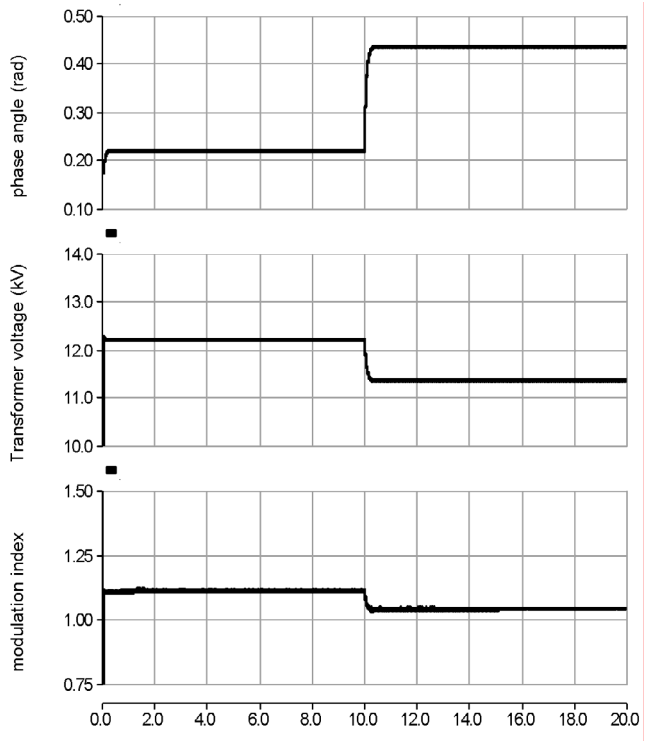

Fig. 14 Control variables from the PQ control system

C. *Power characteristics*

Fig. 15 shows the response of the fuel cell power (P_{fc}), DC/DC converter power (P_o) and the real power injection into the utility grid (P_{ac}). The fuel cell power takes around 5s to reach the new steady value of 90kW. The response of the DC/DC converter is better than that of the fuel cell: it takes around 2.5s to reach the new steady value. The real power flow into the utility grid takes less than 0.1s to reach the new steady state value. The slow response of the SOFC, evident from Fig. 15, is due to the slow change in the chemical reaction parameters after a change in the flow of reactants. The fast transient characteristic of the power electronic devices (DC/DC converter and the DC/AC inverter) has been utilized to improve the fuel cell performance when connected to the grid. Further, the DC link capacitor at the terminals of the DC/DC converter of Fig. 3 provides the extra power required to maintain the power balance between P_{fc} and P_o during the transient period. The difference between P_o and P_{ac} (i.e., the inverter output) during the transient period is made up by the same dc link capacitor; however, because a PI controller controls the inverter output, a faster response is obtained by optimizing the time constant of the integral portion of the controller. Thus, the slow response of the SOFC can be compensated with the help of the power conditioning unit.

The DC/DC converter improves the response by 50%. The response is further improved with the three phase DC/AC inverter. The real power flow into the grid takes less than 0.1s to reach the new steady value of 90 from 50kW. The slow response of the fuel cell prevents it from grid-tie applications. The response time can be improved by 98% with the power conditioning units.

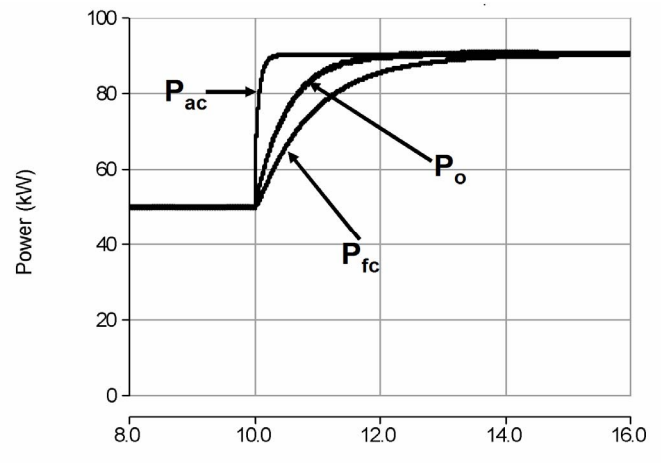

Fig. 15 Power characteristics for a step change in P_{ref}

VI. CONCLUSION

A three phase inverter has been modeled and connected between the SOFC-DC/DC system on one side and the utility grid on the other side through an ideal transformer. A control strategy for the inverter switching signals has been discussed and modeled. The inverter control scheme uses a decoupled PQ control system to control the phase angle of the inverter and the voltage across the transformer. The reactive power injection was taken as zero. The fuel cell and DC/DC converter characteristics have been plotted for a step change in the real reference power. The control variables (phase angle and the voltage) have been obtained from the proposed control scheme. The power characteristics of the entire system have been plotted. A comparison is made between the response of the fuel cell power, DC/DC converter power and the real power flow into the utility grid. The power conditioning unit improves the slow response of the fuel cell. The response time is improved by 50% with the DC/DC converter connected to SOFC. The response time is further improved by an additional 45-48% (i.e. 95-98% overall) with the three phase inverter connection to the SOFC-DC/DC system. Hence the power conditioning unit makes the fuel cell a potential distributed generation resource for grid-tied applications.

APPENDIX

Table 1. System Data

DC/DC voltage (V_O)	600V
Line-line rms grid side voltage (V_{LLrmsu})	12.5kV
Turns ratio of the transformer (K_t)	30.6
Transformer leakage inductance (L_t)	1.76H

REFERENCES

[1] Fuel Cells 2000, *News and Update,* www.fuelcells.org.

[2] N. Akkinapragada and B.H.Chowdhury, "SOFC-based fuel cells for load following stationary applications," *Proceedings of the 38th North American Power Symposium,* pp. 683-690, Sept. 2006.

[3] C. Wang, M.H. Nehrir and H. Gao, "Control of PEM fuel cell distributed generation systems," *IEEE Trans. Energy Conversion,* vol.21, no.2, June 2006.

[4] B. Delfino and F. Fornari, "Modeling and control of an integrated fuel cell-wind turbine system," *IEEE PowerTech Conference, Bologna,* vol.2, June 23-26, Bologna, Italy.

[5] R. Lasseter, "Dynamic models for micro-turbines and fuel cells," *Power Engineering Society, Summer meeting*, vol.2, pp. 761-766, 15-19 July 2001.

[6] K. Sedghisigarchi and A. Feliachi, "Dynamic and transient analysis of power distribution systems with fuel cells Part II: Control and stability enhancement," *IEEE Trans .Energy Conversion*, vol. 19, pp. 429-434, June 2004.

[7] J. Larmine and A Dicks, "Fuel Cell Systems Explained," 2nd Edition, John Wiley & Sons 2003.

[8] Fuel Cells for Distributed Generation, *A Technology and Marketing Summary,* March 2000. www.wisc.edu.

[9] Y. Zhu and K. Tomsovic, "Development of models for analyzing the load-following performance of microturbines and fuel cells," *Electric Power Systems Research 62(2002),* pp.1-11.

[10] N. Mohan, T.M.Undeland and W.P. Robbins, "Power Electronics, Converters, Applications and Design," 2nd Edition, John Wiley & Sons.

[11] P.C. Krause, O. Wasynczuk and S.D. Sudhoff, "Analysis of Electric Machinery and Drives Systems," IEEE Press 2002.

[12] A. Hajimiragha, "Generation control in small isolated power systems," Master of science thesis, Royal Institute of Technology, Stockholm 2005.

BIOGRAPHIES

Nagasmitha Akkinapragada obtained her BE in Electrical Engineering from University college of Engineering, Osmania, Hyderabad, India. She is currently a M.S. candidate in the Electrical & Computer Engineering department of the University of Missouri-Rolla. Her research interests are power system analysis, distributed generation and electric machines and drives.

Badrul H. Chowdhury (M'1983, SM'1993) obtained his Ph.D. degree in Electrical Engineering from Virginia Tech, Blacksburg, VA in 1987. He is currently a Professor in the Electrical & Computer Engineering department of the University of Missouri-Rolla. From 1987 to 1998 he was with the University of Wyoming's Electrical Engineering department. Dr. Chowdhury's research interests are in power system modeling, analysis and control and distributed generation. He teaches courses in power systems, power quality and power electronics.